

Observation of the conversion decay $\phi \rightarrow \pi^0 e^+ e^-$ at CMD-2

R.R. Akhmetshin*, E.V. Anashkin*, M. Arpagaus*,
 V.M. Aulchenko‡, V.Sh. Banzarov*, L.M. Barkov*†,
 N.S. Bashtovoy*, A.E. Bondar*†, D.V. Bondarev*, A.V. Bragin*,
 D.V. Chernyak*, S.I. Eidelman*†, G.V. Fedotovitch*,
 N.I. Gabyshev*, A.A. Grebeniuk*, D.N. Grigoriev*, V.W. Hughes‡,
 F.V. Ignatov*†, P.M. Ivanov*, S.V. Karpov*, V.F. Kazanin*†,
 B.I. Khazin*†, I.A. Koop*, P.P. Krovkovny*†, L.M. Kurdadze*†,
 A.S. Kuzmin*†, M. Lechner*, I.B. Logashenko*, P.A. Lukin*,
 K.Yu. Mikhailov*†, I.N. Nesterenko*, V.S. Okhapkin*,
 A.V. Otboev*, E.A. Perevedentsev*†, A.S. Popov*†, T.A. Purlatz*†,
 N.I. Root*†, A.A. Ruban*, N.M. Ryskulov*, A.G. Shamov*,
 Yu.M. Shatunov*, B.A. Shwartz*†, A.L. Sibidanov*†,
 V.A. Sidorov*, A.N. Skrinsky*, V.P. Smakhtin*, I.G. Snopkov*,
 E.P. Solodov*†, P.Yu. Stepanov*, A.I. Sukhanov*, J.A. Thompson§,
 V.M. Titov*, A.A. Valishev*, Yu.V. Yudin*, S.G. Zverev*

November 13, 2018

Abstract

Using 15.1 pb^{-1} of data collected by CMD-2 in the ϕ -meson energy range, the branching ratio of the conversion decay $\phi \rightarrow \pi^0 e^+ e^-$ has been measured for the first time:

$$B(\phi \rightarrow \pi^0 e^+ e^-) = (1.22 \pm 0.34 \pm 0.21) \cdot 10^{-5}.$$

*Budker Institute of Nuclear Physics, Novosibirsk, 630090, Russia

†Novosibirsk State University, Novosibirsk, 630090, Russia

‡Yale University, New Haven, CT 06511, USA

§University of Pittsburgh, Pittsburgh, PA 15260, USA

1 Introduction

Conversion decays of a vector meson V into a pseudoscalar meson P and a lepton pair l^+l^- ($V \rightarrow Pl^+l^-$, where $l = e, \mu$) are closely related to the corresponding radiative decays of V into P and a photon ($V \rightarrow P\gamma$).

In conversion decays a squared invariant mass of a lepton pair $M_{inv}^2(l^+l^-) = q^2$ or a squared mass of the virtual radiated photon is not equal to zero as for usual radiative decays. By studying $M_{inv}(l^+l^-)$ spectra one can determine a so called transition form factor $F_P(q_1^2, q_2^2)$ of pseudoscalar mesons P as a function of q_i^2 .

Various theoretical models, from standard vector meson dominance (VMD) to calculations on the lattice, predict the transition form factor and the resulting branching ratio of the decay [1, 2, 3, 4].

Precise values of the branching ratios of conversion decays are also important while studying the yield of direct lepton pairs in heavy ion collisions. As it was noted long ago, an observation of the anomalously large yield could indicate the existence of the quark-gluon plasma [5]. In general, both the yield of dileptons and their mass spectra are of interest while studying the change of the meson properties in medium [6]. Recent experiments studying dileptons in heavy ion collisions at CERN reported on an excess of the number of e^+e^- [7] and $\mu^+\mu^-$ pairs [8] over the expectations from usual hadron decays ($\pi^0 \rightarrow e^+e^-\gamma$, $\eta \rightarrow e^+e^-\gamma$, $\eta' \rightarrow e^+e^-\gamma$, $\omega \rightarrow \pi^0e^+e^-$, $\rho/\omega \rightarrow e^+e^-$, $\phi \rightarrow e^+e^-$ as well as similar decays into muon pairs). Its explanation requires the accurate calculation of the production rate of pseudoscalar and vector mesons as well as good knowledge of both the invariant mass spectra and the branching ratios of their decays into lepton pairs.

The experimental information on such decays is rather scarce [9]. While for the ω meson both possible decays into π^0 were observed, $\omega \rightarrow \pi^0\mu^+\mu^-$ [10] and $\omega \rightarrow \pi^0e^+e^-$ [11], only few events of the decay $\phi \rightarrow \eta e^+e^-$ were detected [12].

A large data sample of the ϕ mesons collected by two detectors at VEPP-2M allowed reliable detection of the decay mode $\phi \rightarrow \eta e^+e^-$ by both CMD-2 [13] and SND [14] groups. CMD-2 has also reported on the first observation of the $\phi \rightarrow \pi^0e^+e^-$ decay [13].

This work is devoted to the determination of the branching ratio for the conversion decay $\phi \rightarrow \pi^0e^+e^-$ using the complete data sample available at CMD-2.

2 Experiment

The general purpose detector CMD-2 installed at the e^+e^- collider VEPP-2M [15] has been described in detail elsewhere [16].

It consists of a cylindrical drift chamber (DC) and double-layer multi-wire proportional Z-chamber, both also used for the trigger, and both inside a thin ($0.38 X_0$) superconducting solenoid with a field of 1T. The momentum resolution of the DC is equal to $\sigma_p/p = \sqrt{90 \cdot (p(\text{GeV}))^2 + 7\%}$. The accuracy in the measurement of polar and azimuthal angles is $\sigma_\theta = 1.5 \cdot 10^{-2}$ and $\sigma_\phi = 7 \cdot 10^{-3}$ radians respectively.

The barrel calorimeter with a thickness of $8.1X_0$ is placed outside the solenoid and consists of 892 CsI crystals. The energy resolution for photons is about 9% in the energy range from 50 to 600 MeV. The angular resolution is of the order of 0.02 radians.

The end-cap calorimeter placed inside the solenoid consists of 680 BGO crystals. The thickness of the calorimeter for normally incident particles is equal to $13.4X_0$. The energy and angular resolution varies from 8% to 4% and from 0.03 to 0.02 radians respectively for the photon energy in the range 100 to 700 MeV. Both barrel and end-cap calorimeters cover a solid angle of $0.92 \times 4\pi$ steradians.

The experiment was performed in the ϕ meson energy range (985-1060 MeV). The integrated luminosity collected during the runs of 1993 (PHI93), 1996 (PHI96) and 1998 (PHI98) was 1.5, 2.1 and 11.5 pb^{-1} respectively, so that our analysis is based on the data sample corresponding to 15.1 pb^{-1} .

3 Data analysis

3.1 General approach

A search for events of the decay $\phi \rightarrow \pi^0 e^+ e^-$ used the final state with two charged particles and two photons from the decay $\pi^0 \rightarrow \gamma\gamma$. For the process under study the invariant mass of the two photons $M_{inv}(\gamma\gamma)$ should be equal to the π^0 -mass within the resolution. Event selection was performed using kinematical reconstruction taking into account energy-momentum conservation. The number of detected events is given by:

$$N_{\phi \rightarrow \pi^0 e^+ e^-} = N_\phi \cdot B(\phi \rightarrow \pi^0 e^+ e^-) \cdot B(\pi^0 \rightarrow \gamma\gamma) \cdot \varepsilon_{\phi \rightarrow \pi^0 e^+ e^-} \quad (1)$$

where N_ϕ is the total number of the produced ϕ mesons and $\varepsilon_{\phi \rightarrow \pi^0 e^+ e^-}$ is the corresponding detection efficiency.

One of the most important backgrounds to our process comes from events of the decay $\phi \rightarrow \pi^0\gamma$, $\pi^0 \rightarrow \gamma\gamma$ followed by the γ -quantum conversion at the wall of the beam pipe. Since the DC space resolution is not sufficient to separate events with the conversion at the beam pipe from those due to conversion decays at the interaction point, the contribution of this background was calculated from the simulation:

$$N_{\phi \rightarrow \pi^0\gamma} = N_\phi \cdot B(\phi \rightarrow \pi^0\gamma) \cdot B(\pi^0 \rightarrow \gamma\gamma) \cdot \varepsilon_{\phi \rightarrow \pi^0\gamma}, \quad (2)$$

where $\varepsilon_{\phi \rightarrow \pi^0\gamma}$ is the detection efficiency of the $\phi \rightarrow \pi^0\gamma$ decay with the γ conversion in the material.

Another significant source of background is the decay mode $\phi \rightarrow \pi^+\pi^-\pi^0$. In this case the kinematical reconstruction assuming that charged tracks are electrons, gives $M_{inv}(\gamma\gamma)$ about 150 MeV, i.e. only slightly different from the π^0 -mass, and is not sufficient to separate this process from (1). Therefore, to suppress this background, the procedure of e/π separation by the energy loss of charged particles in the calorimeter was developed (see the next subsection and [17]) allowing determination of the expected number $N_{\phi \rightarrow \pi^+\pi^-\pi^0}$ of such events.

Other sources of background are the quantum electrodynamical (QED) process $e^+e^- \rightarrow e^+e^-\gamma\gamma$, and the decay mode $\phi \rightarrow \eta\gamma$ followed by the Dalitz decay $\eta \rightarrow e^+e^-\gamma$ or the conversion of γ from the $\eta \rightarrow \gamma\gamma$ decay. All these background processes can be separated from the decay under study by their wide and smooth distribution of $M_{inv}(\gamma\gamma)$.

The total number of observed events is a sum of the three contributions above:

$$N_{\phi \rightarrow \pi^0 e^+ e^-}^{exp} = N_{\phi \rightarrow \pi^0 e^+ e^-} + N_{\phi \rightarrow \pi^0 \gamma} + N_{\phi \rightarrow \pi^+ \pi^- \pi^0}. \quad (3)$$

The following selection criteria were used for the decay $\phi \rightarrow \pi^0 e^+ e^-$:

- the impact parameter of the tracks $d < 0.25$ cm to reject events with the $K_{S,L}^0$ decay in DC;
- the angle between two tracks $\Delta\psi < 0.3$ radians to suppress the process $\phi \rightarrow \pi^+\pi^-\pi^0$ (for conversion decays the angle between e^+ and e^- is small);
- the number of photons $N_\gamma^{KREC} = 2$;
- the photon energy $E_\gamma^{max} < 460$ MeV to suppress the process $e^+e^- \rightarrow e^+e^-\gamma\gamma$;
- $E_\gamma^{min} > 50$ MeV for calorimeter noise suppression;

- $|E_\gamma^{max} - 362| > 15$ MeV for suppression of the conversion decay $\eta \rightarrow e^+e^-\gamma$.

To determine the total number of the produced ϕ mesons, events of the process $\phi \rightarrow \eta\gamma$, $\eta \rightarrow \pi^+\pi^-\gamma$ have been used. Since this process also contains two charged particles and two photons in the final state, normalization to it allows to cancel some possible systematic errors. The number of events of this process is given by the following formula:

$$N_{\eta \rightarrow \pi^+\pi^-\gamma} = N_\phi \cdot B(\phi \rightarrow \eta\gamma) \cdot B(\eta \rightarrow \pi^+\pi^-\gamma) \cdot \varepsilon_{\eta \rightarrow \pi^+\pi^-\gamma}. \quad (4)$$

For the normalization process the selection criteria are:

- $\Delta\psi < 2.5$ to suppress $K_S^0 \rightarrow \pi^+\pi^-$ events;
- $N_\gamma^{KREC} = 2$;
- $M_{inv}(\gamma\gamma) > 250$ MeV for suppression of $\phi \rightarrow \pi^+\pi^-\pi^0$ events;
- $d < 0.25$ cm to reject events with the $K_{S,L}^0$ decay in DC.

Figure 1 shows the distribution of the invariant mass $M_{inv}(\pi^+\pi^-\gamma)$ for thus selected experimental events. A clear signal from the process $\phi \rightarrow \eta\gamma$, $\eta \rightarrow \pi^+\pi^-\gamma$ is observed at the η -meson mass. It can be fit with a Gaussian whose variance is taken from simulation. The background mainly comes from events of the process $\phi \rightarrow \eta\gamma$, $\eta \rightarrow \pi^+\pi^-\pi^0$ with a lost photon (the wide signal in the 500 MeV region can be fit with the logarithmic Gaussian [18]), the decay $\phi \rightarrow \pi^+\pi^-\pi^0$ and the QED process $e^+e^- \rightarrow e^+e^-\gamma\gamma$ (another wide background fit with the Gaussian).

Eliminating N_ϕ from the relations (1), (2) and (4), the following expression for the branching ratio of the decay $\phi \rightarrow \pi^0 e^+ e^-$ can be obtained from (3):

$$B(\phi \rightarrow \pi^0 e^+ e^-) = B(\phi \rightarrow \eta\gamma) \cdot \frac{B(\eta \rightarrow \pi^+\pi^-\gamma)}{B(\pi^0 \rightarrow \gamma\gamma)} \cdot \frac{\varepsilon_{\eta \rightarrow \pi^+\pi^-\gamma}}{\varepsilon_{\phi \rightarrow \pi^0 e^+ e^-}} \cdot \frac{N_{\phi \rightarrow \pi^0 e^+ e^-}^{exp} - N_{\phi \rightarrow \pi^+\pi^-\pi^0}}{N_{\eta \rightarrow \pi^+\pi^-\gamma}} - B(\phi \rightarrow \pi^0\gamma) \cdot \frac{\varepsilon_{\phi \rightarrow \pi^0\gamma}}{\varepsilon_{\phi \rightarrow \pi^0 e^+ e^-}} \quad (5)$$

Here $N_{\phi \rightarrow \pi^+\pi^-\pi^0}$ is the expected number of the events of the decay $\phi \rightarrow \pi^+\pi^-\pi^0$ obtained from the procedure of e/π separation.

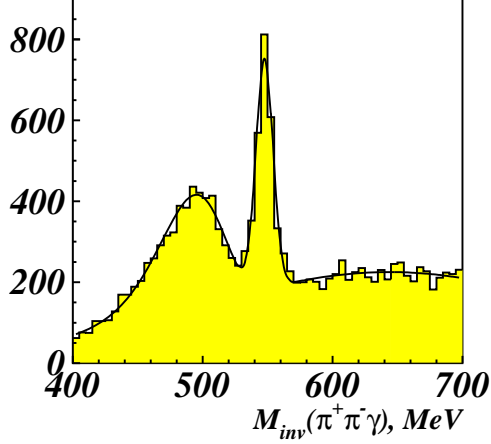


Figure 1: Invariant mass $M_{inv}(\pi^+\pi^-\gamma)$ for $\phi \rightarrow \eta\gamma$, $\eta \rightarrow \pi^+\pi^-\gamma$

3.2 e/π -separation

Since simulation can not completely reproduce interactions of charged particles with the calorimeter, the procedure of e/π -separation is based on the experimental data. Energy losses of e^\pm and π^\pm were studied using “clean” samples of events of the processes $e^+e^- \rightarrow e^+e^-\gamma$ and $\phi \rightarrow \pi^+\pi^-\pi^0$, $\pi^0 \rightarrow \gamma\gamma$ respectively. The QED process $e^+e^- \rightarrow e^+e^-\gamma$ with small angles between the tracks was chosen as the closest to $\phi \rightarrow \pi^0 e^+e^-$.

From the distributions of E/P (the energy loss of a charged particle in the calorimeter divided by its momentum in DC) versus P shown in Fig. 2 a) for pions from the $\phi \rightarrow \pi^+\pi^-\pi^0$ decay and in Fig. 2 b) for electrons from the $e^+e^- \rightarrow e^+e^-\gamma$ it can be seen that e/π can be separated well.

The whole region of momenta from 0 to 500 MeV was divided to bins 50 MeV wide and for each bin the E/P distributions were plotted. These spectra were fit by: for e^\pm – the logarithmic Gaussian function, for π^\pm – a sum of two standard Gaussian functions. A probability to penetrate the detector without any energy loss and a probability to lose some energy in the calorimeter were defined as a ratio of the number of events with $E = 0$ and with $E > 0$ to the total number of events respectively.

Then the probability density functions for each sort of the particles f_{e^\pm, π^\pm} depend on the momentum in DC and energy loss in the calorimeter.

The probability for one track to be π^+ or π^- :

$$W_{\pi^+} = \frac{f_{\pi^+}}{f_{\pi^+} + f_{e^+}}, \quad W_{\pi^-} = \frac{f_{\pi^-}}{f_{\pi^-} + f_{e^-}} \quad (6)$$

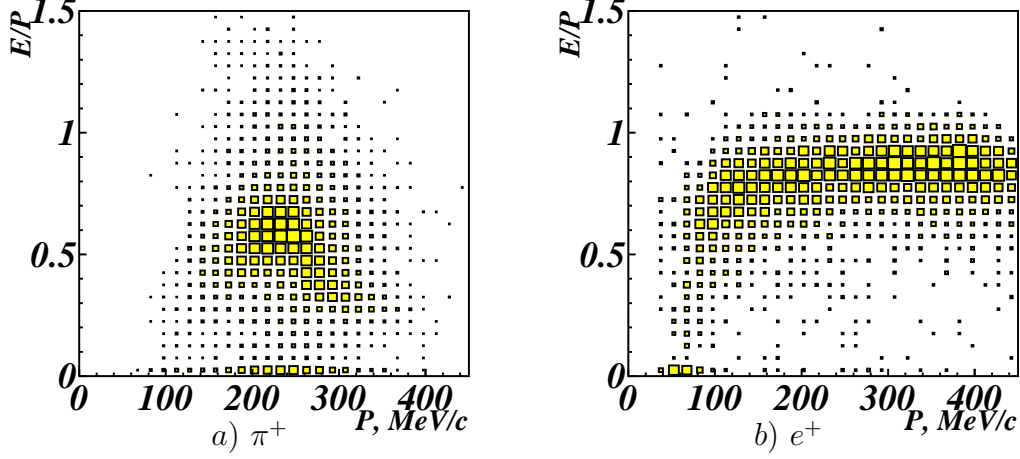


Figure 2: Distribution of E/P vs P : a) π^+ for $\phi \rightarrow \pi^+\pi^-\pi^0$; b) e^+ for $e^+e^- \rightarrow e^+e^-\gamma$

The probability for one track to be e^+ or e^- :

$$W_{e^+} = \frac{f_{e^+}}{f_{\pi^+} + f_{e^+}}, \quad W_{e^-} = \frac{f_{e^-}}{f_{\pi^-} + f_{e^-}} \quad (7)$$

Similarly, one can construct the probability for both tracks in the event to be $\pi^+\pi^-$ or e^+e^- :

$$W_{\pi^+\pi^-} = \frac{W_{\pi^+} \cdot W_{\pi^-}}{W_{\pi^+} \cdot W_{\pi^-} + W_{e^+} \cdot W_{e^-}}, \quad W_{e^+e^-} = \frac{W_{e^+} \cdot W_{e^-}}{W_{\pi^+} \cdot W_{\pi^-} + W_{e^+} \cdot W_{e^-}} \quad (8)$$

Finally, we can determine the detection efficiencies $\varepsilon_{e^+e^-}^{e/\pi}$ and $\varepsilon_{\pi^+\pi^-}^{e/\pi}$ which respectively give the probability to detect an e^+e^- and $\pi^+\pi^-$ pair as an e^+e^- one. They are calculated as the ratio of the number of events with $W_{e^+e^-} > W_0$ to the total number of sample events of the processes $e^+e^- \rightarrow e^+e^-\gamma$ and $\phi \rightarrow \pi^+\pi^-\pi^0$ respectively. Here W_0 is some boundary value chosen from the analysis of the $W_{e^+e^-}$ distribution.

3.3 Selection of $\phi \rightarrow \pi^0 e^+ e^-$ events

The main selection criteria for the process under study were listed above.

Figure 3 shows the scatter plot of the probability $W_{e^+e^-}$ for both tracks to be electrons versus the invariant mass of the photons $M_{inv}(\gamma\gamma)$ for the PHI98 data after these cuts. Events with an e^+e^- -pair have $W_{e^+e^-} \sim 1$ while for those with pions $W_{e^+e^-} \sim 0$. Events in the region $W_{e^+e^-} \sim 0$ and $M_{inv}(\gamma\gamma) \sim 150$ MeV come from the decay $\phi \rightarrow \pi^+\pi^-\pi^0$. To suppress it, the additional cut based on the e/π -separation was applied:

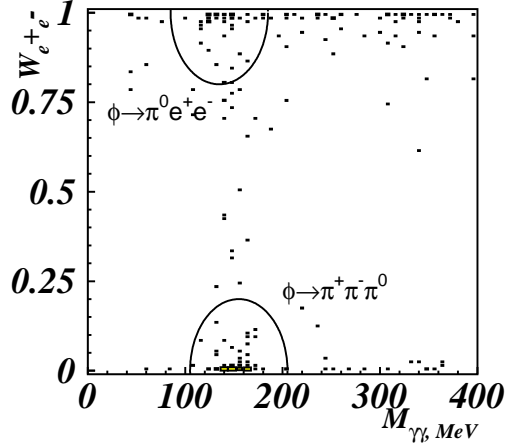


Figure 3: Scatter plot of $W_{e^+e^-}$ versus $M_{inv}(\gamma\gamma)$

- $W_{e^+e^-} > 0.5$, the probability that an event has an e^+e^- -pair.

Figure 4 shows the distribution of the invariant mass $M_{inv}(\gamma\gamma)$ for the data after this selection. A clear signal is observed at the π^0 -meson mass which can be fit with a Gaussian (its variance is taken from simulation). The wide background can be also fit with a Gaussian.

If instead the cut $W_{e^+e^-} > 0.5$ one applies the complementary cut

- $W_{e^+e^-} < 0.5$, to enhance the probability that the event has a $\pi^+\pi^-$ pair,

the expected number $N_{\phi \rightarrow \pi^+\pi^-\pi^0}$ can be determined.

Detection efficiencies were determined from the Monte Carlo simulation (MC) [19] taking into account the efficiencies of e/π separation $\varepsilon_{e^+e^-}^{e/\pi}, \varepsilon_{\pi^+\pi^-}^{e/\pi}$ and a correction $\varepsilon_{\Delta\Psi}$ for the reconstruction of events with a small opening angle, for brevity referred to as the small angle correction. The reconstruction of such events can not be completely reproduced by the simulation and was therefore specially studied using experimental events of the process $\phi \rightarrow \pi^+\pi^-\pi^0, \pi^0 \rightarrow e^+e^-\gamma$ which also have a small angle between an electron and positron.

$$\varepsilon_{\phi \rightarrow \pi^0 e^+ e^-} = \varepsilon_{\phi \rightarrow \pi^0 e^+ e^-}^{MC} \cdot \varepsilon_{\Delta\Psi} \cdot \varepsilon_{e^+e^-}^{e/\pi}, \quad \varepsilon_{\phi \rightarrow \pi^0 \gamma} = \varepsilon_{\phi \rightarrow \pi^0 \gamma}^{MC} \cdot \varepsilon_{\Delta\Psi} \cdot \varepsilon_{e^+e^-}^{e/\pi},$$

$$\varepsilon_{\phi \rightarrow \pi^+\pi^-\pi^0} = \varepsilon_{\phi \rightarrow \pi^+\pi^-\pi^0}^{MC} \cdot \varepsilon_{\Delta\Psi} \cdot \varepsilon_{\pi^+\pi^-}^{e/\pi}.$$

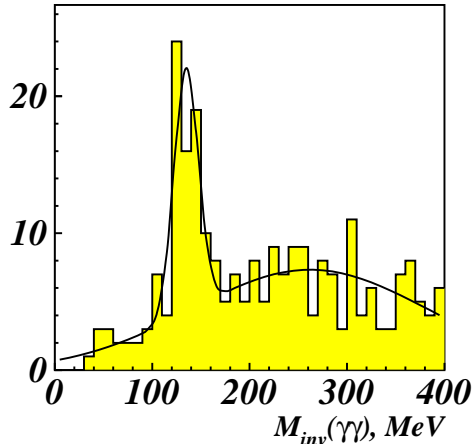


Figure 4: The invariant mass $M_{inv}(\gamma\gamma)$ for $\phi \rightarrow \pi^0 e^+ e^-$, $\pi^0 \rightarrow \gamma\gamma$

4 Results

Figure 5 shows the energy dependence of the visible cross section of the process $\phi \rightarrow \pi^0 e^+ e^-$, $\pi^0 \rightarrow \gamma\gamma$ for the run PHI98. It is compatible with that expected for the ϕ meson, but a small non-resonant background can not be excluded. In fact, one should expect such a background coming from the "tail" of the $\omega \rightarrow \pi^0 e^+ e^-$ decay. To determine the number of events coming from the ϕ meson decay, a fit of the visible cross section was performed which included a Breit-Wigner signal of the ϕ meson and a possible non-resonant background. The fit with the ϕ meson mass and width fixed at their world average values gave the following ratio of the non-resonant background cross section to that at the peak

$$\frac{\sigma_{\omega}}{\sigma_{\phi}} = 7.5^{+15.4\%}_{-7.5\%}$$

compatible with the VMD estimate. From this value as well as from the integrated luminosity one can determine the corrected number of events for the process under study:

$$N_{\phi \rightarrow \pi^0 e^+ e^-}^{exp} = 47.6 \pm 11.1.$$

Similar analysis was performed for the data of PHI93 and PHI96 runs.

Table 1 presents the final results of the data processing: the number of selected events, the expected number of events of $\phi \rightarrow \pi^0 e^+ e^-$, $\phi \rightarrow \pi^0 \gamma$ and $\phi \rightarrow \pi^+ \pi^- \pi^0$ determined by the described procedure, the detection efficiencies and branching ratios of the $\phi \rightarrow \pi^0 e^+ e^-$ decay in various runs. Also

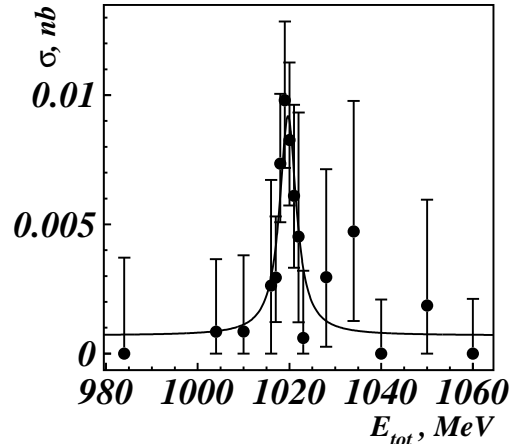


Figure 5: The visible cross section of $\phi \rightarrow \pi^0 e^+ e^-$, $\pi^0 \rightarrow \gamma\gamma$ versus the total energy

presented in the Table are the data for the normalization process. The differences of the efficiencies from run to run are caused by varying conditions of data taking. The total detected number of the $\phi \rightarrow \pi^0 e^+ e^-$ candidates is 67.9 ± 12.3 with an expected background of 22.3 ± 1.4 events. The error in the estimated number of background events is determined by the procedure described above.

As already noted, since the number of events of the process under study is normalized to that of the process $\phi \rightarrow \eta\gamma$, $\eta \rightarrow \pi^+\pi^-\gamma$ with a similar final state, some of the systematic uncertainties cancel (trigger, detection efficiencies etc.).

The main sources of the remaining systematic errors are listed below, their magnitude given for the most statistically significant run PHI98:

- A limited sample of simulated events used to determine detection efficiencies - 2.7%
- Statistical errors of the parameters in the small angle correction - 3.9%
- Parameters of the e/π separation procedure - 2.5%
- The shape of the invariant mass distributions used in the fits - 11.9%
- Inaccurate knowledge of the thickness of material in front of the DC (the beryllium beam pipe and the DC inner wall made of aluminized mylar) - 2.2%

Table 1: Branching ratio of $\phi \rightarrow \pi^0 e^+ e^-$ decay

Run	PHI93	PHI96	PHI98	Total
$N_{\phi \rightarrow \pi^0 e^+ e^-}^{exp}$	6.3 ± 2.8 ± 0.1	14.1 ± 4.4 ± 0.5	47.6 ± 11.1 ± 3.6	67.9 ± 12.3 ± 5.2
$\varepsilon_{\pi^0 e^+ e^-}^{MC}, \%$	19.11 ± 0.31 ± 2.18	26.74 ± 0.37 ± 2.51	23.10 ± 0.34 ± 1.82	
$\varepsilon_{\pi^0 \gamma}^{MC}, 10^{-4}$	4.98 ± 0.22 ± 0.40	7.30 ± 0.27 ± 0.59	5.44 ± 0.23 ± 0.44	
$\varepsilon_{\Delta\Psi}, \%$	99.5 ± 20.1 ± 7.1	91.0 ± 10.4 ± 5.6	96.4 ± 2.8 ± 4.7	
$\varepsilon_{e^+ e^-}^{e/\pi}, \%$	92.4 ± 8.3	93.3 ± 5.4	89.9 ± 1.3	
$\varepsilon_{\pi^+ \pi^-}^{e/\pi}, \%$	9.1 ± 2.9	7.8 ± 1.0	7.0 ± 0.4	
Expected $N_{\phi \rightarrow \pi^0 \gamma}$	0.9 ± 0.3 ± 0.1	2.2 ± 0.3 ± 0.3	8.5 ± 0.6 ± 1.1	11.7 ± 0.7 ± 1.5
Expected $N_{\pi^+ \pi^- \pi^0}$	1.4 ± 0.6 ± 0.1	1.7 ± 0.5 ± 0.1	7.4 ± 1.0 ± 0.1	10.6 ± 1.3 ± 0.1
Total expected background	2.3 ± 0.7	4.0 ± 0.6	16.0 ± 1.1	22.3 ± 1.4
Expected $N_{\phi \rightarrow \pi^0 e^+ e^-}$	3.9 ± 2.9	10.1 ± 4.4	31.6 ± 11.2	45.6 ± 12.4
$\varepsilon_{\eta \rightarrow \pi^+ \pi^- \gamma}, \%$	12.34 ± 0.25	20.47 ± 0.32	20.75 ± 0.32	
$N_{\eta \rightarrow \pi^+ \pi^- \gamma}$	126 ± 17 ± 6	362 ± 25 ± 9	1858 ± 58 ± 38	2346 ± 65 ± 53
$B(\phi \rightarrow \pi^0 e^+ e^-), 10^{-5}$	1.36 ± 1.13 ± 0.22	1.57 ± 0.75 ± 0.23	1.10 ± 0.40 ± 0.19	1.22 ± 0.34 ± 0.21

- The shape of the distributions used in the fits to determine the parameters of the small angle correction - 6.8%
- Errors of the world average values for the branching ratios of intermediate decays from [9] - 4.9%
- Dependence on the transition form factor model. The form factor in the generalized VMD ($\rho + \rho'$ mesons) was compared to that in the simple VMD (single ρ meson only). The contribution to the branching ratio is 9.5%.

Three first sources of the error are of statistical nature, their values were

obtained for each run separately, so that they are uncorrelated. Their total contribution to the error is 5.4% and can be quadratically added to the statistical error. All others are obviously correlated from run to run and their total magnitude is 17.5%.

From the last line of Table 1 it is clear that the values of the branching ratio obtained in different runs are consistent within the errors. To improve the accuracy, we can average them. The resulting value of the branching ratio for the $\phi \rightarrow \pi^0 e^+ e^-$ decay is $(1.22 \pm 0.34 \pm 0.21) \cdot 10^{-5}$ where the first error is statistical (including the uncorrelated systematic errors discussed above) and the second one is a systematic correlated error common for all runs.

5 Conclusion

For the first time the branching ratio of the conversion decay $\phi \rightarrow \pi^0 e^+ e^-$ has been determined by the CMD-2 detector at VEPP-2M:

$$B(\phi \rightarrow \pi^0 e^+ e^-) = (1.22 \pm 0.34 \pm 0.21) \cdot 10^{-5}. \quad (9)$$

This measurement is based on 68 selected candidates for the events of the process $\phi \rightarrow \pi^0 e^+ e^-$ with an expected background of 22 events. The obtained value agrees with the theoretical predictions $(1.3 - 1.6) \cdot 10^{-5}$ [4, 20, 21] and with the experimental upper limit $1.2 \cdot 10^{-4}$ at 90% CL placed by the neutral detector ND at VEPP-2M using a data sample of 2.8 pb^{-1} [11]. Our result supersedes the previous value of $(0.85 \pm 0.61 \pm 0.12) \cdot 10^{-5}$ obtained by CMD-2 and based on a data sample corresponding to 1.5 pb^{-1} only [22].

The applied procedure of event selection and particularly the cut on the angle between the tracks $\Delta\Psi < 0.3$ selects events with a rather small q^2 so that it is practically impossible to study the momentum transfer dependence of the cross section. Therefore, one can conclude that the study of transition form factors will become feasible when much larger data samples are collected.

The authors are grateful to the staff of VEPP-2M for the excellent performance of the collider, to all engineers and technicians who participated in the design, commissioning and operation of CMD-2. We acknowledge useful comments of V.P. Druzhinin and stimulating discussions with R.A. Eichler.

REFERENCES

1. L. Landsberg, Phys. Rep. **128** (1985) 301.

2. A. Bramon, M. Greco, The Second DAΦNE Physics Handbook. INFN-Laboratori Nazionali di Frascati. Edited by L.Maiani, G.Pancheri, N.Paver. 1995. Vol.2, p.451.
3. M. Crisafulli, V. Lubicz, The Second DAΦNE Physics Handbook. INFN-Laboratori Nazionali di Frascati. Edited by L.Maiani, G.Pancheri, N.Paver. 1995. Vol.2, p.515.
4. A. Faessler, C. Fuchs and M.I. Krivoruchenko, Phys. Rev. **C61** (2000) 035206.
5. E.V. Shuryak, Phys. Lett. **B78** (1978) 150.
6. S.A. Chin, Ann. Phys. (N.Y.) **108** (1977) 301.
7. G. Agakichiev *et al.*, Phys. Rev. Lett. **75** (1995) 1272.
8. M. Masera, Nucl. Phys. **A590** (1995) 93c.
9. D.E. Groom *et al.*, Eur. Phys. J. **C15** (2000) 1.
10. R.I. Dzhelyadin *et al.*, Phys. Lett. **84B** (1979) 143.
11. S.I. Dolinsky *et al.*, Sov. J. Nucl. Phys. **48** (1988) 277.
12. V.B. Golubev *et al.*, Sov. J. Nucl. Phys. **41** (1985) 756.
13. E.P. Solodov, Proceedings of the VII Int. Conf. on Hadron Spectroscopy, Upton, NY, 1997, AIP Conf. Proceed. 432, p.778.
14. M.N. Achasov *et al.*, Preprint BudkerINP 98-65, Novosibirsk, 1998.
15. V.V. Anashin *et al.*, Preprint Budker INP 84-114, Novosibirsk, 1984.
16. G.A. Aksenov *et al.*, Preprint Budker INP 85-118, Novosibirsk, 1985.
E.V. Anashkin *et al.*, ICFA Instr. Bulletin **5** (1988) 18.
17. R.R. Akhmetshin *et al.*, Phys. Lett. **B475** (2000) 190.
18. Handbook of Applicable Mathematics, Volume VI: Statistics, John Wiley and Sons, 1984.
19. E.V. Anashkin *et al.*, Preprint Budker INP 99-1, Novosibirsk, 1999.
20. S. Eidelman, Proceedings of the Workshop on Physics and Detectors for DAΦNE, Frascati, 1991, p.451.
21. M. Hashimoto, Phys. Rev. **D54** (1996) 5611.
22. M. Lechner, Dissertation Swiss Federal Institute of Technology (ETH) for Doctor of Natural Science degree, Diss. ETH No. 12866 and ETHZ-IPP Internal Report 98-5.